

Research Article



An *in vitro* model of *Fusobacterium nucleatum* and *Porphyromonas gingivalis* in single- and dual-species biofilms

Lívia Jacovassi Tavares , Marlise Inêz Klein , Beatriz Helena Dias Panariello ,
Erica Dorigatti de Avila , Ana Cláudia Pavarina

Department of Dental Materials and Prosthodontics, São Paulo State University - UNESP School of Dentistry at Araraquara, Araraquara, Sao Paulo, Brazil



Received: Dec 12, 2017
Accepted: Feb 10, 2018

*Correspondence:

Ana Cláudia Pavarina

Department of Dental Materials and Prosthodontics, São Paulo State University - UNESP School of Dentistry at Araraquara, Rua Humaitá, 1680, Araraquara 14801-903, Brasil.

E-mail: pavarina@foar.unesp.br

Tel: +55-16-3301-6424

Fax: +55-16-3301-6406

Copyright © 2018. Korean Academy of Periodontology
This is an Open Access article distributed under the terms of the Creative Commons Attribution Non-Commercial License (<https://creativecommons.org/licenses/by-nc/4.0/>).

ORCID iDs

Lívia Jacovassi Tavares
<https://orcid.org/0000-0002-5338-1228>
Marlise Inêz Klein
<https://orcid.org/0000-0002-7916-1557>
Beatriz Helena Dias Panariello
<https://orcid.org/0000-0002-2138-1223>
Erica Dorigatti de Avila
<https://orcid.org/0000-0001-6681-1269>
Ana Cláudia Pavarina
<https://orcid.org/0000-0002-9231-1994>

Funding

This work was supported by the Coordination for the Improvement of Higher Level or Education Personnel (CAPES), the National Council for Scientific and Technological Development (CNPq), and the CEPID/CEPOF (Research, Innovation and Diffusion Centers/

ABSTRACT

Purpose: The goal of this study was to develop and validate a standardized *in vitro* pathogenic biofilm attached onto saliva-coated surfaces.

Methods: *Fusobacterium nucleatum* (*F. nucleatum*) and *Porphyromonas gingivalis* (*P. gingivalis*) strains were grown under anaerobic conditions as single species and in dual-species cultures. Initially, the bacterial biomass was evaluated at 24 and 48 hours to determine the optimal timing for the adhesion phase onto saliva-coated polystyrene surfaces. Thereafter, biofilm development was assessed over time by crystal violet staining and scanning electron microscopy.

Results: The data showed no significant difference in the overall biomass after 48 hours for *P. gingivalis* in single- and dual-species conditions. After adhesion, *P. gingivalis* in single- and dual-species biofilms accumulated a substantially higher biomass after 7 days of incubation than after 3 days, but no significant difference was found between 5 and 7 days. Although the biomass of the *F. nucleatum* biofilm was higher at 3 days, no difference was found at 3, 5, or 7 days of incubation.

Conclusions: Polystyrene substrates from well plates work as a standard surface and provide reproducible results for *in vitro* biofilm models. Our biofilm model could serve as a reference point for studies investigating biofilms on different surfaces.

Keywords: Bacterial adhesion; Biofilms; *Fusobacterium nucleatum*; *Porphyromonas gingivalis*

INTRODUCTION

Periodontal and peri-implant diseases are infections associated with complex biofilm structures that induce an inflammatory response, causing the destruction of connective tissue [1,2]. The prevalence of periodontitis in adults is approximately 47% [3], making it the sixth most prevalent oral disease [4], while peri-implantitis was found to be present in 28% of subjects examined in a previous study [5]. *Porphyromonas gingivalis* is a red complex anaerobic Gram-negative bacterium, strongly associated with the advancement of both types of oral infection [6-8]. The mechanisms involved in bacterial colonization of natural and artificial surfaces, as well as the surrounding periodontal tissues, include direct attachment

Research Center for Optics and Photonics) under grant No. 2013/072761.

Author Contributions

Conceptualization: Lívia Jacovassi Tavares, Marlise Inêz Klein, Ana Cláudia Pavarina; Data curation: Lívia Jacovassi Tavares, Marlise Inêz Klein, Beatriz Helena Dias Panariello, Erica Dorigatti de Avila; Formal analysis: Lívia Jacovassi Tavares, Erica Dorigatti de Avila; Methodology: Lívia Jacovassi Tavares, Beatriz Helena Dias Panariello, Erica Dorigatti de Avila; Project administration: Ana Cláudia Pavarina; Writing - original draft: Lívia Jacovassi Tavares, Marlise Inêz Klein, Beatriz Helena Dias Panariello, Ana Cláudia Pavarina; Writing - review & editing: Marlise Inêz Klein, Erica Dorigatti de Avila, Ana Cláudia Pavarina.

Conflict of Interest

No potential conflict of interest relevant to this article was reported.

to saliva proteins and epithelial cell receptors, and/or interactions with early bacterial colonizers [9-12]. *Fusobacterium nucleatum* is also a Gram-negative bacterium, and is regarded as a central organism for dental biofilm maturation due to its wide ability to coaggregate with other microorganisms, such as *P. gingivalis* [13-16]. This pattern of coaggregation, which is known to be mutually beneficial, promotes the expression of a high number of virulence factors by both species [17]. Virulence factors may contribute to the survival, presence, and pathogenicity of these microorganisms in various oral niches [13,18]. Once bacteria are attached to a surface, the dynamic interactions between the host and the bacteria evolve into an organized and complex microbial community, protected from mechanical and chemical damage [19]. The development of promising strategies for fighting oral infections requires *in vitro* models of mature biofilms, which are useful for purposes such as obtaining a better understanding of the mechanism of action of certain drugs. Such models are essential for evaluating the efficiency of therapies that aim to control and prevent oral diseases caused by pathogenic biofilms.

In the scientific literature, studies have reported various *in vitro* biofilm models used to assess the effects of specific materials, as well as to investigate the efficacy of treatments [20-23]. However, there is limited knowledge regarding the time period necessary for establishing a mature biofilm. Although oral biofilms are typically polymicrobial, mixed biofilms constructed with selected microbial species allow controlled *in vitro* assays, which enable a better understanding of the impact of materials and/or new treatments on pathogenic species [24-26]. Our purpose in this study was to develop a pathogenic dual-species biofilm model with *P. gingivalis* and *F. nucleatum* to use in further *in vitro* research. The contribution of each bacterium to the maturity of the biofilm was investigated through comparisons with the corresponding single-species biofilms. In this model, bacteria were grown on human saliva-coated surfaces to simulate oral conditions and to enhance bacterial attachment [27,28].

MATERIALS AND METHODS

Preparation of saliva

Human saliva samples from 3 healthy adult male volunteers were collected on ice, with the approval of the Ethics Committee for Research in Humans (CAAE 26142014.0.0000.5416) and after informed consent was obtained. None of the participants had been treated for oral diseases or had taken any prescription medication during the 3 months before the study [29]. For standardization, all saliva was collected at the same time of day. The saliva was prepared as described in previous studies [30]. Before its use, the supernatant obtained after centrifugation at 45 N for 15 minutes at 4°C was purified with a 0.22 µm membrane filter (Millipore, Burlington, MA, USA) and stored at -80°C [31,32].

Bacteria and growth conditions

The pathogenic bacteria strains used in this study were *F. nucleatum* NCTC 11326 and *P. gingivalis* ATCC 32277. The microorganisms stored at -80°C were seeded onto Brucella agar (HiMedia, Mumbai, India) prepared with 5% sheep blood (Microlab, Shenzhen, China) and kept at 37°C, inside an anaerobic incubator with an oxygen-free atmosphere (85% N₂, 10% H₂, 5% CO₂) (Don Whitley, Shipley, England). After 48 hours of incubation, the microorganism colonies were transferred to 10 mL of brain heart infusion (BHI; Difco™, BD, Rutherford, NJ, USA) broth medium, supplemented with hemin (10 mg/mL) and menadione (5 mg/mL), and maintained at 37°C under anaerobic conditions for 24 hours. Then, 500 µL of bacterial cells

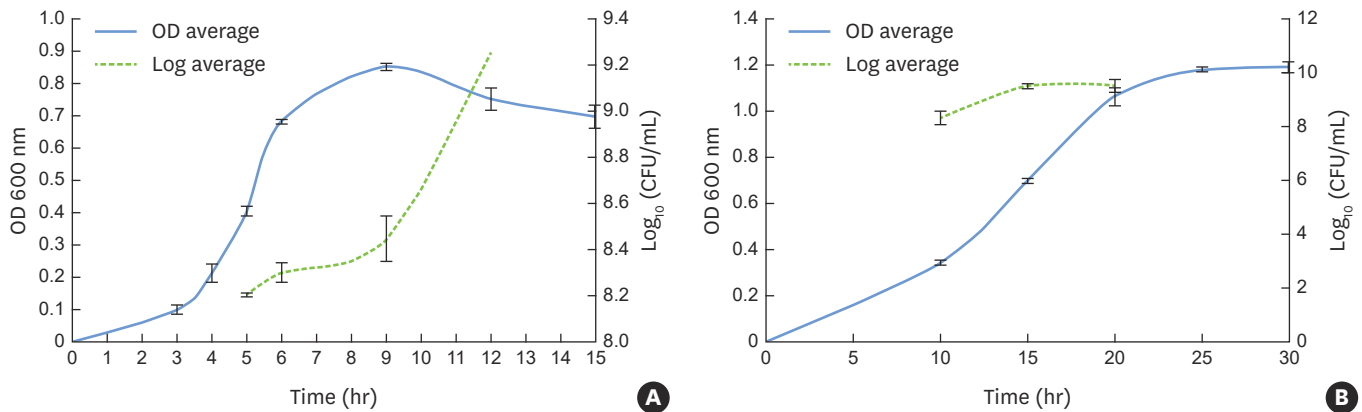


Figure 1. Growth curves represented by OD at 600 nm and CFU/mL for *F. nucleatum* NCTC 11326 (OD, 0.4±0.01; 8.2±0.007 CFU/mL) (A) and *P. gingivalis* ATCC 33277 (OD, 0.7±0.01; 9.5±0.1 CFU/mL) (B) at the mid-log phase. OD: optical density, CFU: colony-forming units.

was transferred to 9.5 mL of fresh BHI medium and the tubes were incubated in the same conditions described above until the mid-exponential growth phase, which occurred after 5 hours for *F. nucleatum* and 15 hours for *P. gingivalis* (Figure 1). The bacterial cell concentrations were estimated by determining the optical density at 600 nm (spectrophotometer spectrum – SP 2000 UV, Wildlife Supply, Yulee, FL, USA). When the mid-log phase was reached, each inoculum was diluted to obtain a final concentration of 1×10^7 colony-forming units (CFU)/mL in BHI fresh media for assays of bacterial adhesion and subsequent biofilm formation.

Adhesion and biofilm formation in 96-well microliter plates

The initial step involved acquired pellicle formation. In this step, 50 μ L of saliva was placed into each 96-well plate (TPP tissue culture, TPP, Trasadingen, Switzerland) and maintained at 37°C in an orbital shaker (75 rpm) [33]. After 4 hours of incubation, excess saliva was removed and the wells were rinsed twice with 100 μ L of sterile phosphate-buffered saline (PBS; 100 mM NaCl, 100 mM NaH_2PO_4 , pH 7.2). Next, we investigated whether 24 or 48 hours after incubation was the best time point for the adhesion of the bacterial cells. In this step, 150 μ L of the mid-exponential phase bacterial suspensions (1×10^7 CFU/mL for both *P. gingivalis* and *F. nucleatum*) was added into each 96-well plate and then incubated at 37°C under anaerobic conditions. After the incubation period for adhesion, the medium was removed, the wells were washed gently twice with 200 μ L of PBS to eliminate unattached bacteria, and 150 μ L of fresh supplemented BHI medium was added to the biofilm formation assay. Biofilm maturation was evaluated at 3, 5 and 7 days, corresponding to the respective experimental times for biomass accumulation (Figure 2). The culture medium was changed every 24 hours.

Biomass by crystal violet staining

The biomass of adhered bacteria and accumulated biofilm on the polystyrene plates was determined by crystal violet staining. After the established periods, the culture medium was removed, and 50 μ L of 0.1% crystal violet solution was added to each well. After 15 minutes at room temperature, the solution was removed and each well was carefully washed twice with 350 μ L of PBS to remove the excess dye. Then, 200 μ L of 99% ethanol was pipetted into each well and the plate was maintained for 15 minutes at room temperature. The solution containing the eluted crystal violet stain was transferred onto a new micro-plate to estimate the overall biomass. The experiment was performed in triplicate with 4 repetitions to ensure methodological and biological reproducibility.

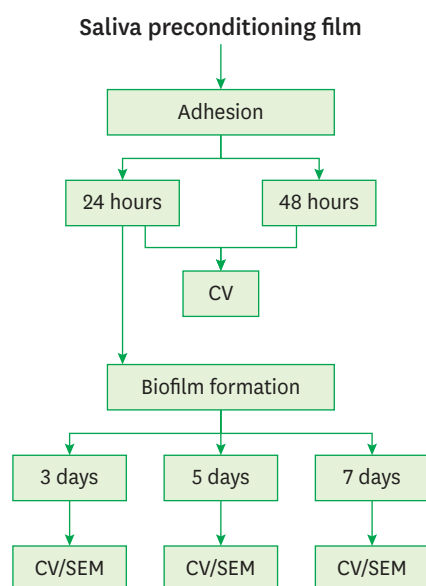


Figure 2. Schematic presentation of the sequence of experiments.
 CV: crystal violet, SEM: scanning electron microscopy.

Scanning electron microscopy (SEM)

Samples for assessing the maturation of the biofilms were cultured on sterile polystyrene discs on a 24-well plate (TPP tissue culture, TPP) in single- and dual-species conditions. After 3, 5, or 7 days of incubation, the discs were rinsed twice with 1 mL of sterile 0.89% sodium chloride solution and prepared for SEM analysis. A solution of 2.5% glutaraldehyde (pH 7.4) was used to fix the samples at room temperature for 1 hour followed by a standard graded series of ethanol solutions to dehydrate the specimens: 70% and 90% ethanol for 60 minutes per step, ending with 5 changes within 30 seconds of 100% ethanol. Before visualization, the discs were kept under vacuum to guarantee that the samples were moisture-free, and after being stored for 7 days, the polystyrene discs were sputter-coated with gold. Images at high magnification ($\times 3,500$) were taken of different areas of the discs with SEM (JEOL JSM-6610LV, JEOL, Tokyo, Japan). SEM was performed in 2 samples of single- and dual-species biofilms for each time point on 2 different occasions.

Statistical analysis

The 1-tailed unpaired *t*-test was used to establish the best time point for the adhesion period. For biofilm formation, 1-way analysis of variance with the Tukey *post hoc* test was employed to analyze differences within the previously established periods. Before performing other statistical procedures, the D'Agostino-Pearson normality test was applied to assess the normality of the data distribution ($\alpha=0.05$). A normal distribution was not confirmed for *P. gingivalis* in the single-species biofilms, so the Kruskal-Wallis test followed by Dunn multiple comparison was required.

RESULTS

Prior the experiments, the growth curves of both species of pathogenic bacteria were constructed to standardize the bacterial concentrations, and the exponential phase was considered to be representative of the cellular proliferation period.

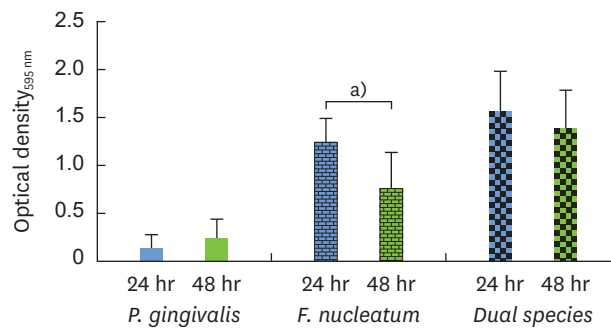


Figure 3. The adhesion phase was evaluated via quantitative measurements of crystal violet staining as an indicator of biomass accumulation after incubation for 24 hours (blue bar) in comparison to 48 hours (green bar). OD: optical density.
^{a)}Indicates a statistically significant difference ($P < 0.05$).

For the adhesion phase, both bacteria were cultured in single- and dual-species setups at 2 different time points. The crystal violet assay revealed a statistically significant difference in overall bacterial attachment for *F. nucleatum* under single-species conditions, with 1.6 times more biomass after 24 hours than after 48 hours, which may have corresponded to a highly proliferative phase of adhesion development. Since no difference was observed between adhesion after 24 and 48 hours for single-species *P. gingivalis* or for the dual-species setup, the 24-hour time point was chosen for the adhesion phase for both *P. gingivalis* and *F. nucleatum* (Figure 3).

Then, the growth of *F. nucleatum* and *P. gingivalis* in single- and dual-species biofilms was examined over time. For *P. gingivalis* in single- and dual-species (*F. nucleatum*+*P. gingivalis*) biofilms, the accumulated biomass was considerably higher after 7 days of incubation than after 3 days, but no significant difference was found between 5 and 7 days for *P. gingivalis* in single-species biofilms. In contrast, the proliferative phase of the *F. nucleatum* biofilm was more predominant at an earlier time point, consistent with the bacterial biomass findings in the adhesion step. When *F. nucleatum* and *P. gingivalis* bacteria were grown in a dual-species biofilm, more biomass was found than in the single-species biofilms, underscoring the close interactions between these bacterial species (Figure 4). The outcomes of crystal violet staining were consistent with the SEM analyses. *P. gingivalis* alone formed an early biofilm, showing well-spaced microcolonies of cells, but without a complex structure at 3 days (Figure 5D, yellow arrow). In contrast, *F. nucleatum* in single- and dual-species biofilms exhibited several

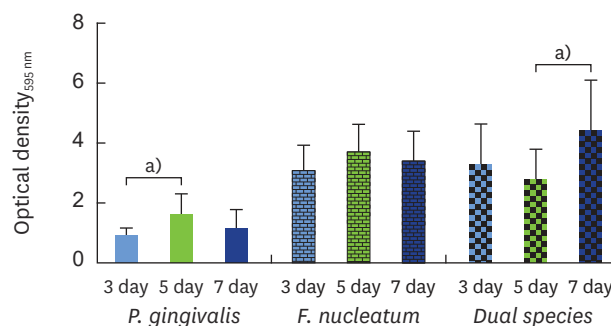


Figure 4. Biofilm formation was evaluated via quantitative measurements of crystal violet staining as an indicator of biomass accumulation after incubation for 3 days (blue bar) in comparison to 5 (green bar) and 7 days (navy bar). OD: optical density.
^{a)}Indicates a statistically significant difference ($P < 0.05$).

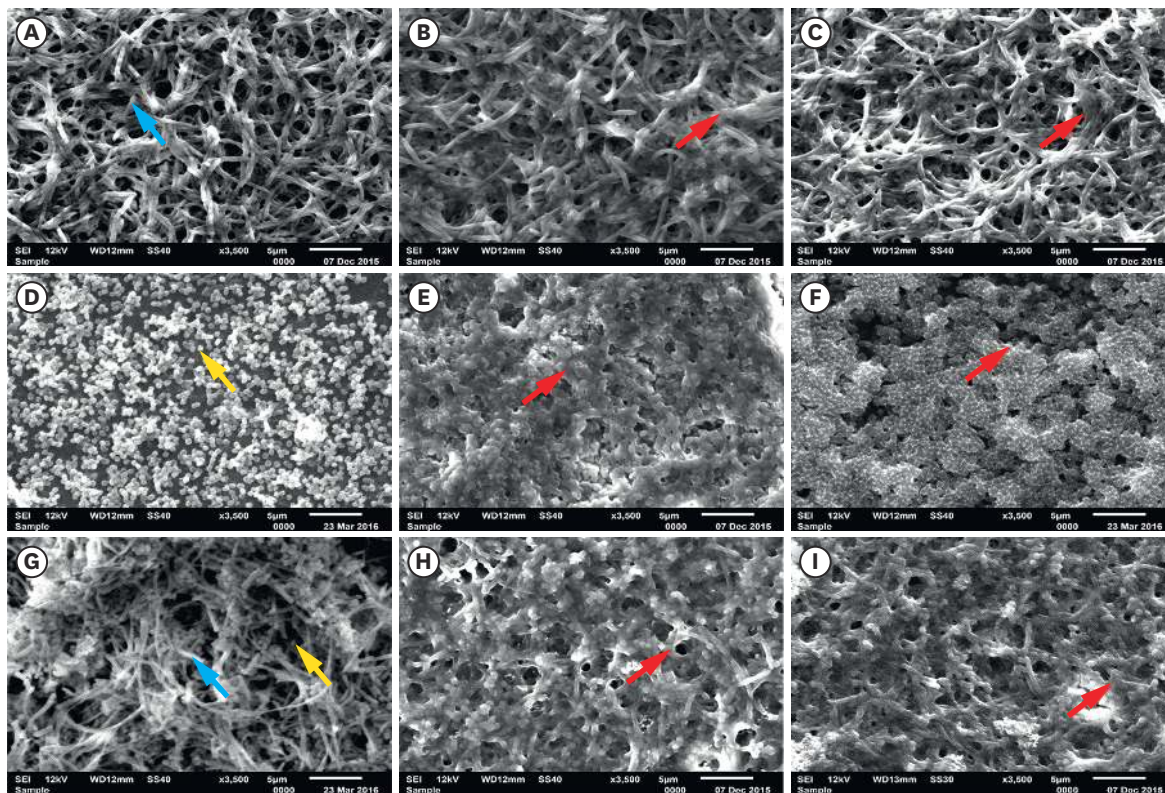


Figure 5. SEM images of single- and dual-species biofilms: *F. nucleatum*: (A) 3 days, (B) 5 days, (C) 7 days; *P. gingivalis*: (D) 3 days, (E) 5 days, (F) 7 days; and dual-species (G) 3 days, (H) 5 days, (I) 7 days (blue arrow, *F. nucleatum*; yellow arrow, *P. gingivalis*; red arrow, biomass; bar=5 μm). SEM: scanning electron microscopy.

dense conglomerates of bacterial cells and a greater area of coverage (Figure 5A and G, blue arrow). Moreover, extracellular matrix could be seen enmeshing the cells. In both the single- and dual-species biofilms, the amount of bacterial cells on the polystyrene discs increased over time, and the increase in the biomass was more evident after 5 days of incubation (Figure 5B, C, E, F, H, and I, red arrow).

DISCUSSION

The success of microbiological experiments depends primarily on using the appropriate methodology to construct biofilms that respond better to *in vitro* investigations. Hence, the goal of this study was to present a clear step-by-step protocol for generating a robust *in vitro* pathogenic biofilm attached onto saliva-coated surfaces. Our data clearly documented the stages of bacterial growth in the planktonic state, and we defined the appropriate time point for the adhesion phase and subsequent steps of biofilm development.

The bacteria concentration used for *in vitro* experiments must be standardized according to the growth curve. The bacterial growth period selected for experimental studies can obscure or interfere with the real outcomes. A growth curve includes 5 critical phases of development: the lag, exponential, stationary, death, and long-term stationary phases [34,35]. The duration of each phase is affected by various factors, primarily involving the quality of the growth culture medium, which can affect metabolic conditions. For *in vitro*

experiments investigating bacterial susceptibility to antimicrobial agents, for example, the variability of the bacterial growth phase should be further evaluated and standardized for quantitative testing [36]. In general, the exponential phase is preferred for experimental investigations, since this period is characterized by increased metabolic activity and cell proliferation. In this study, growth was carefully monitored, using absorbance measurements of each bacterium, before designing the biofilm model. Additionally, the concentrations of CFU per milliliter at the mid-log phase were also determined. The data collected consistently showed that *F. nucleatum* grew earlier than *P. gingivalis*. After 5 hours of incubation in broth medium, *F. nucleatum* had already reached the exponential phase, whereas *P. gingivalis* required 15 hours to do so.

The adhesion phases for both species of bacteria in single- and dual-species setups were then investigated by culturing the bacteria at the concentration found in the exponential phase on saliva-coated polystyrene well plates. The amount of bacterial biomass that was deposited onto the surfaces showed no difference between 24 and 48 hours of incubation for either the single-species *P. gingivalis* or the dual-species biofilms. However, the biomass of *F. nucleatum* in the single-species setups was significantly higher at the earlier time point. Thus, 48 hours of incubation led to a decreased biomass of attached *F. nucleatum*, indicating that there was no or slow growth and possibly cell death, as has been previously discussed [17]. This behavior can be explained by the rapid consumption of nutrients by *F. nucleatum*, as the peak of growth was found in the first 24 hours.

In the oral cavity and *in vitro* models, bacterial cells irreversibly interact with natural and/or artificial substrates, or with each other, and initiate biofilm formation by extracellular polymeric matrix production. In this study, differences in biofilm development were found when *P. gingivalis* and *F. nucleatum* were grown in single-species setups. *P. gingivalis* exhibited slower growth and the biomass of biofilm showed only an early stage of development after 3 days of incubation. The quantitative data were also supported by microscopic images, which showed spread-out high-density areas of condensed cells that did not cover the entire surface. In contrast, *F. nucleatum* produced intricate networks after 3 days, which increased in size after 5 days of incubation, demonstrating a mature biofilm at this stage. Additionally, incubation for 5 or 7 days was not associated with any differences in biomass or 3-dimensional architecture. The same pattern was identified in the dual-species biofilm, indicating that *F. nucleatum* facilitated *P. gingivalis* growth based on positive interactions [12,15,16].

The methodologies used in this study successfully allowed a protocol to be developed for generating single- and dual-species pathogenic biofilms. However, since the bacteria and subsequent biofilms were grown on polystyrene surfaces, our findings might not translate into dental material substrates. We must consider that the physicochemical properties of each type of material influence the amount of bacteria that adhere to and form biofilms on it [21,37-40]; therefore, different bacterial behavior is expected on different substrates. Conversely, a growth reference for the bacterial species involved in a specific study is needed before performing a reliable *in vitro* experiment. Indeed, polystyrene substrates from well plates work as a standard surface and provide reproducible results for *in vitro* biofilm models. Thus, to obtain a better understanding of bacterial behavior and growth, our biofilm model was developed on the bottom of polystyrene plates. The *in vitro* biofilms described herein could serve as a reference point for studies investigating biofilms on different surfaces.

REFERENCES

1. Malcolm J, Millington O, Millhouse E, Campbell L, Adrados Planell A, Butcher JP, et al. Mast cells contribute to *Porphyromonas gingivalis*-induced bone loss. *J Dent Res* 2016;95:704-10.
[PUBMED](#) | [CROSSREF](#)
2. Feng X, Zhu L, Xu L, Meng H, Zhang L, Ren X, et al. Distribution of 8 periodontal microorganisms in family members of Chinese patients with aggressive periodontitis. *Arch Oral Biol* 2015;60:400-7.
[PUBMED](#) | [CROSSREF](#)
3. Eke PI, Dye BA, Wei L, Thornton-Evans GO, Genco RJ. Prevalence of periodontitis in adults in the United States: 2009 and 2010. *J Dent Res* 2012;91:914-20.
[PUBMED](#) | [CROSSREF](#)
4. Marcenes W, Kassebaum NJ, Bernabe E, Flaxman A, Naghavi M, Lopez A, et al. Global burden of oral conditions in 1990–2010: a systematic analysis. *J Dent Res* 2013;92:592-7.
[PUBMED](#) | [CROSSREF](#)
5. Zitzmann NU, Berglundh T. Definition and prevalence of peri-implant diseases. *J Clin Periodontol* 2008;35:286-91.
[PUBMED](#) | [CROSSREF](#)
6. Socransky SS, Haffajee AD. Periodontal microbial ecology. *Periodontol* 2000 2005;38:135-87.
[PUBMED](#) | [CROSSREF](#)
7. How KY, Song KP, Chan KG. *Porphyromonas gingivalis*: an overview of periodontopathic pathogen below the gum line. *Front Microbiol* 2016;7:53.
[PUBMED](#) | [CROSSREF](#)
8. van Winkelhoff AJ, Loos BG, van der Reijden WA, van der Velden U. *Porphyromonas gingivalis*, *Bacteroides forsythus* and other putative periodontal pathogens in subjects with and without periodontal destruction. *J Clin Periodontol* 2002;29:1023-8.
[PUBMED](#) | [CROSSREF](#)
9. Periasamy S, Kolenbrander PE. Mutualistic biofilm communities develop with *Porphyromonas gingivalis* and initial, early, and late colonizers of enamel. *J Bacteriol* 2009;191:6804-11.
[PUBMED](#) | [CROSSREF](#)
10. Tribble GD, Kerr JE, Wang BY. Genetic diversity in the oral pathogen *Porphyromonas gingivalis*: molecular mechanisms and biological consequences. *Future Microbiol* 2013;8:607-20.
[PUBMED](#) | [CROSSREF](#)
11. Kirschbaum M, Schultze-Mosgau S, Pfister W, Eick S. Mixture of periodontopathic bacteria influences interaction with KB cells. *Anaerobe* 2010;16:461-8.
[PUBMED](#) | [CROSSREF](#)
12. Saito A, Kokubu E, Inagaki S, Imamura K, Kita D, Lamont RJ, et al. *Porphyromonas gingivalis* entry into gingival epithelial cells modulated by *Fusobacterium nucleatum* is dependent on lipid rafts. *Microb Pathog* 2012;53:234-42.
[PUBMED](#) | [CROSSREF](#)
13. Feuille F, Ebersole JL, Kesavalu L, Stepfen MJ, Holt SC. Mixed infection with *Porphyromonas gingivalis* and *Fusobacterium nucleatum* in a murine lesion model: potential synergistic effects on virulence. *Infect Immun* 1996;64:2094-100.
[PUBMED](#)
14. Metzger Z, Lin YY, Dimeo F, Ambrose WW, Trope M, Arnold RR. Synergistic pathogenicity of *Porphyromonas gingivalis* and *Fusobacterium nucleatum* in the mouse subcutaneous chamber model. *J Endod* 2009;35:86-94.
[PUBMED](#) | [CROSSREF](#)
15. Diaz PI, Zilm PS, Rogers AH. *Fusobacterium nucleatum* supports the growth of *Porphyromonas gingivalis* in oxygenated and carbon-dioxide-depleted environments. *Microbiology* 2002;148:467-72.
[PUBMED](#) | [CROSSREF](#)
16. Ahn SH, Song JE, Kim S, Cho SH, Lim YK, Kook JK, et al. NOX1/2 activation in human gingival fibroblasts by *Fusobacterium nucleatum* facilitates attachment of *Porphyromonas gingivalis*. *Arch Microbiol* 2016;198:573-83.
[PUBMED](#) | [CROSSREF](#)
17. Periasamy S, Chalmers NI, Du-Thumm L, Kolenbrander PE. *Fusobacterium nucleatum* ATCC 10953 requires *Actinomyces naeslundii* ATCC 43146 for growth on saliva in a three-species community that includes *Streptococcus oralis* 34. *Appl Environ Microbiol* 2009;75:3250-7.
[PUBMED](#) | [CROSSREF](#)

18. Ebersole JL, Feuille F, Kesavalu L, Holt SC. Host modulation of tissue destruction caused by periodontopathogens: effects on a mixed microbial infection composed of *Porphyromonas gingivalis* and *Fusobacterium nucleatum*. *Microb Pathog* 1997;23:23-32.
[PUBMED](#) | [CROSSREF](#)
19. Kumada Y, Benson DR, Hillemann D, Hosted TJ, Rochefort DA, Thompson CJ, et al. Evolution of the glutamine synthetase gene, one of the oldest existing and functioning genes. *Proc Natl Acad Sci U S A* 1993;90:3009-13.
[PUBMED](#) | [CROSSREF](#)
20. Amoroso PF, Adams RJ, Waters MG, Williams DW. Titanium surface modification and its effect on the adherence of *Porphyromonas gingivalis*: an *in vitro* study. *Clin Oral Implants Res* 2006;17:633-7.
[PUBMED](#) | [CROSSREF](#)
21. de Avila ED, Avila-Campos MJ, Vergani CE, Spolidorio DM, Mollo Fde A Jr. Structural and quantitative analysis of a mature anaerobic biofilm on different implant abutment surfaces. *J Prosthet Dent* 2016;115:428-36.
[PUBMED](#) | [CROSSREF](#)
22. de Avila ED, Lima BP, Sekiya T, Torii Y, Ogawa T, Shi W, et al. Effect of UV-photofunctionalization on oral bacterial attachment and biofilm formation to titanium implant material. *Biomaterials* 2015;67:84-92.
[PUBMED](#) | [CROSSREF](#)
23. Montelongo-Jauregui D, Srinivasan A, Ramasubramanian AK, Lopez-Ribot JL. An *in vitro* model for oral mixed biofilms of candida albicans and *Streptococcus gordonii* in synthetic saliva. *Front Microbiol* 2016;7:686.
[PUBMED](#) | [CROSSREF](#)
24. Barros J, Grenho L, Fontenente S, Manuel CM, Nunes OC, Melo LF, et al. *Staphylococcus aureus* and *Escherichia coli* dual-species biofilms on nanohydroxyapatite loaded with CHX or ZnO nanoparticles. *J Biomed Mater Res A* 2017;105:491-7.
[PUBMED](#) | [CROSSREF](#)
25. Liu Y, Busscher HJ, Zhao B, Li Y, Zhang Z, van der Mei HC, et al. Surface-adaptive, antimicrobially loaded, micellar nanocarriers with enhanced penetration and killing efficiency in staphylococcal biofilms. *ACS Nano* 2016;10:4779-89.
[PUBMED](#) | [CROSSREF](#)
26. Malaikozhundan B, Vaseeharan B, Vijayakumar S, Pandiselvi K, Kalanjiam MA, Murugan K, et al. Biological therapeutics of *Pongamia pinnata* coated zinc oxide nanoparticles against clinically important pathogenic bacteria, fungi and MCF-7 breast cancer cells. *Microb Pathog* 2017;104:268-77.
[PUBMED](#) | [CROSSREF](#)
27. Badihi Hauslich L, Sela MN, Steinberg D, Rosen G, Kohavi D. The adhesion of oral bacteria to modified titanium surfaces: role of plasma proteins and electrostatic forces. *Clin Oral Implants Res* 2013;24 Suppl A100:49-56.
[PUBMED](#) | [CROSSREF](#)
28. Kohavi D, Klinger A, Steinberg D, Mann E, Sela NM. Alpha-amylase and salivary albumin adsorption onto titanium, enamel and dentin: an *in vivo* study. *Biomaterials* 1997;18:903-6.
[PUBMED](#) | [CROSSREF](#)
29. Moura JS, da Silva WJ, Pereira T, Del Bel Cury AA, Rodrigues Garcia RC. Influence of acrylic resin polymerization methods and saliva on the adherence of four Candida species. *J Prosthet Dent* 2006;96:205-11.
[PUBMED](#) | [CROSSREF](#)
30. Pereira-Cenci T, Cury AA, Cenci MS, Rodrigues-Garcia RC. *In vitro* Candida colonization on acrylic resins and denture liners: influence of surface free energy, roughness, saliva, and adhering bacteria. *Int J Prosthodont* 2007;20:308-10.
[PUBMED](#)
31. Sánchez MC, Llama-Palacios A, Blanc V, León R, Herrera D, Sanz M. Structure, viability and bacterial kinetics of an *in vitro* biofilm model using six bacteria from the subgingival microbiota. *J Periodontal Res* 2011;46:252-60.
[PUBMED](#) | [CROSSREF](#)
32. Thein ZM, Samaranyake YH, Samaranyake LP. Characteristics of dual species Candida biofilms on denture acrylic surfaces. *Arch Oral Biol* 2007;52:1200-8.
[PUBMED](#) | [CROSSREF](#)
33. Ciandrini E, Campana R, Federici S, Manti A, Battistelli M, Falcieri E, et al. *In vitro* activity of Carvacrol against titanium-adherent oral biofilms and planktonic cultures. *Clin Oral Investig* 2014;18:2001-13.
[PUBMED](#) | [CROSSREF](#)

34. Navarro Llorens JM, Tormo A, Martinez-Garcia E. Stationary phase in gram-negative bacteria. *FEMS Microbiol Rev* 2010;34:476-95.
[PUBMED](#) | [CROSSREF](#)
35. Rolfe MD, Rice CJ, Lucchini S, Pin C, Thompson A, Cameron AD, et al. Lag phase is a distinct growth phase that prepares bacteria for exponential growth and involves transient metal accumulation. *J Bacteriol* 2012;194:686-701.
[PUBMED](#) | [CROSSREF](#)
36. Kim KS, Anthony BF. Importance of bacterial growth phase in determining minimal bactericidal concentrations of penicillin and methicillin. *Antimicrob Agents Chemother* 1981;19:1075-7.
[PUBMED](#) | [CROSSREF](#)
37. de Avila ED, de Molon R, Vergani CE, Mollo FA Jr, Salih V. The relationship between biofilm and physical-chemical properties of implant abutment materials for successful dental implants. *Materials (Basel)* 2014;7:3651-62.
[PUBMED](#) | [CROSSREF](#)
38. de Avila ED, de Molon R, Spolidorio DM, Mollo FA Jr. Implications of surface and bulk properties of abutment implants and their degradation in the health of periodontal tissue. *Materials (Basel)* 2013;6:5951-66.
[PUBMED](#) | [CROSSREF](#)
39. de Avila ED, Vergani CE, Mollo Junior FA, Junior MJ, Shi W, Lux R. Effect of titanium and zirconia dental implant abutments on a cultivable polymicrobial saliva community. *J Prosthet Dent* 2017;118:481-7.
[PUBMED](#) | [CROSSREF](#)
40. de Avila ED, de Molon RS, Lima BP, Lux R, Shi W, Junior MJ, et al. Impact of physical chemical characteristics of abutment implant surfaces on bacteria adhesion. *J Oral Implantol* 2016;42:153-8.
[PUBMED](#) | [CROSSREF](#)